

Assessment of some failure criteria for strongly anisotropic geomaterials

G. Duveau, J. F. Shao* and J. P. Henry

Laboratoire de Mécanique de Lille, URA CNRS 1441, EUDIL, Cité Scientifique, 59655 Villeneuve d'Ascq, France

SUMMARY

This paper is devoted to the assessment of some representative failure criteria in the framework of modelling the failure behaviour of strongly anisotropic geomaterials. Experimental data concerning the failure behaviour of a typical strongly anisotropic rock; the schist of Angers are first presented. Nine widely used failure criteria are then selected and classified into three groups, the mathematical continuous models, the empirical continuous models and the discontinuous weakness planes based models. This classification is made up according to the main assumptions and techniques used in each criterion to describe the strength anisotropy. The calibration of each one is carried out with respect to the laboratory data of Angers schist. Qualitative and quantitative comparisons between the selected criteria and with the experimental data are provided. © 1998 John Wiley & Sons, Ltd.

Mech. Cohes.-Frict. Mater. 3: 1–26 (1998)

KEY WORDS: anisotropy; failure criterion; schist; sedimentary rock; rock joints; laboratory testing

1. INTRODUCTION

Many rocks are characterized by a structural inherent anisotropy which is related to the existence of rock fabric elements such as bedding, layering, foliation and lamination planes, or the existence of linear structures. This intrinsic anisotropy should be accounted for in the mechanical behaviour of rocks. The influence of the intrinsic anisotropy on rock failure strength is one of the basic data required for predicting rock performance for a variety of surface and underground structures. The term 'failure strength' is here used to denote either the stress state at which brittle rupture of the sample occurs, or the peak stress attained during large ductile deformation. Laboratory tests with various loading paths have to be performed to determine the general form of failure surface. For anisotropic rocks, the most classical experiment is the conventional triaxial compression test, with various loading orientations and confining pressures (Figure 1). A lot of laboratory studies have been performed on sedimentary rocks (Donath;^{1–3} Donath and Cohen;⁴ Dayre and Sirieys;⁵ Hoek;^{6–8} Chenevert and Gatlin;⁸ McLamore and Gray;¹⁰ Attewell and Sandford;¹¹ Saint Leu, Leran and Sirieys;¹² Alliot and Boehler;¹³ Syries;¹⁴ Lerau, Saint Leu and Sirieys;¹⁵ Niandou *et al.*;¹⁶ etc.). All the results obtained have shown that the rock strength varies with the loading orientation. The maximum strengths are generally found when the axial compressive stress is nearly normal or parallel

* Correspondence to: J. F. Shao, Laboratoire de Mécanique de Lille, URA CNRS 1441, EUDIL, Cité Scientifique, 59655 Villeneuve d'Ascq, France.

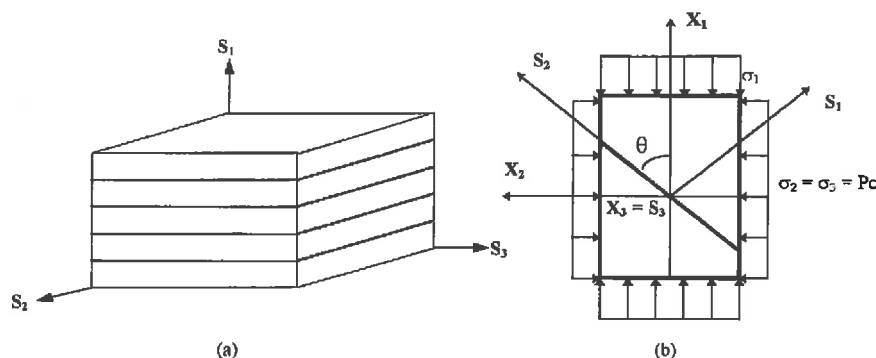


Figure 1. (a) Fixed structural co-ordinate system; (b) definition of loading orientation θ in a triaxial test

to bedding planes. The minimum strength is obtained when the angle between the major stress and bedding planes is located from 30° to 60° . Furthermore, the failure mode in anisotropic rocks depends also on the loading orientation.

Various failure criteria for anisotropic materials have been proposed. However, according to the assumptions and techniques used in each one, it appears possible to classify these criteria into three groups. A tentative classification of some commonly used criteria is proposed in Table I.

The first group of criteria is called mathematical continuous approach. In these criteria, a continuous body is considered and a continuous variation of strength is assumed. The strength anisotropy of material is generally described by using a mathematical technique along with the kind of material symmetries. One of the first anisotropic criteria of this kind was proposed by Hill¹⁷ for frictionless materials by extending the von Mises isotropic theory. A more general approach was proposed by Goldenblat and Kopnov.¹⁸ These authors suggested the use of strength tensors of different order to

Table I. Classification of widely used anisotropic failure criteria

Continuous criteria		
Mathematical approach	Empirical approach	Discontinuous criteria
<ul style="list-style-type: none"> • Von Mises⁵¹ • Hill¹⁷ • Olszak and Urbanowicz⁵² • Goldenblat⁵³ • Goldenblat and Kopnov¹⁸ • Bohler and Sawczuk^{21,22} • Tsa and Wu¹⁹ • Pariseau²⁰ • Bohler²⁵ • Dafalias^{54,55} • Alliro and Bohler¹³ • Nova and Sacchi⁵⁶ • Nova^{57,58} • Bohler and Raclin²⁴ • Raclin⁵⁹ • Kaar <i>et al.</i>⁶⁰ • Cazacu²⁶ 	<ul style="list-style-type: none"> • Casagrande and Carillo⁶¹ • Jaeger (variable cohesive) strength theory³⁰ • McLamore and Gray¹⁰ • Ramamurthy, Rao and Singh²⁸ 	<ul style="list-style-type: none"> • Jaeger (single plane of weakness theory)³⁰ • Walsh and Brace³² • Murrell⁶² • Hoek⁶⁻⁸ • Barron⁶³ • Ladanyi and Archambault⁶⁴ • Bieniawski⁶⁵ • Hoek and Brown^{33,34} • Duveau and Henry³⁵

take into account the anisotropy. A failure criterion which uses strength tensors of first and second order was proposed by Tsai and Wu.¹⁹ For geological materials, a widely used criterion was proposed by Pariseau²⁰ by modifying the Hill criterion, in order to take into account the strength difference in tensile and compressive loading and the strength dependency on the mean stress. Parallel to these works, a more rigorous and general approach was developed by Boehler and Sawczuk^{21,22} and Boehler²³ in the framework of the theory of invariant tensorial functions. Specific failure criteria were also proposed for rock materials (Alliot and Boehler¹³), and for composites (Boehler and Raclin²⁴). Generalizations of Mohr–Coulomb and von Mises isotropic failure criteria to orthotropic and transversely isotropic media can be found in Boehler.²⁵ More recently, a new invariant failure criterion was developed by Cazacu²⁶ by extending the Stassi isotropic criterion.

The criteria of the second group are named empirical continuous models. Indeed, the strength anisotropy is simply described by the determination of variation laws as a function of the loading orientation for some material parameters used in an isotropic criterion. Such variation laws are fully empirical in nature and calibrated from a simple fitting of experimental data. Any clear physical and mathematical background is not included in these models. One of the representative criteria of this kind was proposed by Jaeger,²⁷ known as ‘the variational cohesion theory’, who extended the Mohr–Coulomb failure criterion by using a variable material cohesion with the loading orientation and a constant value of the friction. A simple modification of this criterion was proposed by McLamore and Gray¹⁰ who proposed to use a variation of the friction coefficient in the same way as the cohesion. Ramamurthy, Rao and Singh,²⁸ and Singh, Ramamurthy and Rao²⁹ proposed a modification of the McLamore and Gray criterion by using a non-linear form of the failure envelope in Mohr plane.

In contrast to the previous two groups of criteria, a third group of criteria was developed and called ‘discontinuous weakness planes based’ models. In these theories, the emphasis is put on the description of physical mechanisms included in the failure process. The basic assumption is that the failure of an anisotropic body is due to either the fracture of bedding planes or the fracture of the rock matrix and two distinct criteria should be used for the two fracture modes. The most representative model of this kind was proposed by Jaeger,³⁰ known as ‘the single plane of weakness theory’. By considering the planes of weakness as orientated Griffith cracks and based on the extension of the modified Griffith theory (McClintock and Walsh³¹), some other criteria were proposed (Walsh and Brace;³² Hoek and Brown,^{33,34} Hoek⁸). More recently, a new theory was proposed by Duveau and Henry³⁵ who proposed to use the Barton criterion for sliding along schistosity planes.

In this paper, a particular anisotropic rock, a schist from Angers (France), is investigated. Experimental studies have been performed on this material (Hamade, Morel and Henry;³⁶ Hamade;³⁷ Homand *et al.*³⁸) under the co-ordination of the ANDRA (French National Agency for Radioactive Waste Management). The results obtained have shown specific failure modes of this material due to its particular anisotropic structure. Indeed, the structure of this material is characterized by a set of clearly defined schistosity planes, which plays a dominant role in the mechanical behaviour of the material. The material failure is due to sliding of schistosity planes for a large range of loading orientations (from 10 to 80 degrees). The failure strength is almost constant in this range of loading orientations. This kind of strong strength anisotropy marks a significant difference from most sedimentary rocks reported in previous works. In these rocks, a continuous smooth variation of failure strength was obtained and the rupture by sliding of bedding planes was not the dominant mechanism.

The present paper focuses on the assessment and comparison of some representative criteria in the framework of modelling of failure behaviour of strongly anisotropic rocks. A summary of experimental data obtained from the schist of Angers is first presented. The emphasis is put on the failure behaviour of the material. Nine representative criteria of different groups are then selected. Basic assumptions and techniques used in each criterion are presented and compared. Quantitative comparisons of numerical simulations obtained from each model with the experimental data are provided.

2. SUMMARY OF EXPERIMENTAL INVESTIGATIONS

The studied material is a middle Ordovician schist from Angers (France). It is a rock of the family of schists with weak metamorphism, and characterized by well marked schistosity planes which coincide with the stratification planes. The main mineral constituents of this rock are chlorite, muscovite and quartz. Small quantities of pyrite, calcite and chloritoid are also found. The size of grains varies from 10 to 20 μm . The testing program reported in this paper is composed of preliminary tests for the analysis of structural anisotropy, triaxial tests for the variations of failure strength with loading orientation and confining pressure. Table II sums up the testing programme used.

2.1. Preliminary studies

Preliminary tests were performed to determine the degree of structural anisotropy of the material. It consisted of measuring wave velocities along the identified structural axes of the rock, as illustrated in Figure 2. After the results obtained by Cuxac,³⁹ the smallest wave velocity was found in the direction S_1 normal to the schistosity planes, while the highest one is associated with one direction parallel to the schistosity planes. However, the velocities measured along two orthogonal directions (S_2, S_3) in the schistosity planes were slightly different. Such a difference may be related to secondary linear structure apart from the main bedding planes. Accordingly, two anisotropy degrees can be defined, the major one noted as ΔM and the minor one noted as Δm . These anisotropy coefficients are generally calculated from the following equations (Guyader and Denis⁴⁰):

$$\Delta M\% = 100 \left[1 - \frac{2V_1}{V_2 + V_3} \right] \quad \Delta m\% = 100 \left[\frac{2(V_3 - V_2)}{V_2 + V_3} \right] \quad (1)$$

where V_1, V_2 and V_3 are the velocities in the three structural axes. For the schist studied, three tests were performed on different cubic samples and the values of the major and minor anisotropy coefficients obtained are given in Table III. We can clearly notice that the minor anisotropy of the schist is much smaller than the major one. Therefore, it appears reasonable to assume that this schist has a transversely isotropic structure. Hydrostatic compression tests were also performed by Hamade³⁷ on the same material. Strains in the three structural axes have been measured and are shown in Figure 3. We can see that the strain in the direction S_1 , normal to the bedding planes, is much higher than those in the directions (S_2, S_3), parallel to the bedding planes. In addition, the strains in the two orthogonal directions (S_2, S_3) are quasi-identical. This results is in good agreement

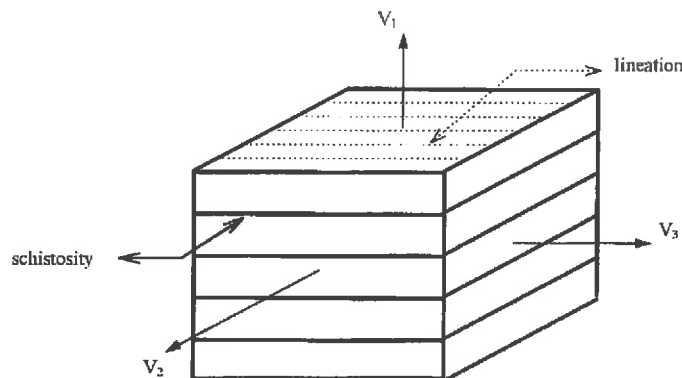


Figure 2. Measuring directions of the wave velocity (from Homand *et al.*³⁸)

Table II. List of the laboratory tests performed on the schist studied and used in this paper

Preliminary tests	3 Ultrasonic measurement tests 1 Hydrostatic compressibility test						
	Loading orientation θ	Confining pressure σ_3 (MPa)					
		0	5	10	20	30	40
Triaxial tests	0°	2	1	1	2	2	3
	10°	—	—	—	1	—	—
	13°	—	—	1	—	—	—
	15°	1	1	1	2	2	—
	16°	—	3	—	—	1	2
	30°	3	2	2	1	1	1
	45°	2	1	2	2	1	1
	60°	1	1	3	1	1	1
	74°	1	—	—	—	—	—
	75°	—	—	1	2	—	—
	76°	—	—	—	—	1	1
	77°	—	1	—	1	—	1
	78°	1	1	1	1	1	—
	90°	2	2	1	2	2	2

with the wave velocity measurement and confirms the assumption of the transversely isotropic behaviour of the schist.

2.2. Failure behaviour in triaxial compression tests

A large laboratory investigation project has been achieved on the Angers schist. Detailed experimental data can be found in Hamade, Morel and Henry,³⁶ Hamade³⁷ and Homand *et al.*³⁸ 78 triaxial compression tests have been performed for loading orientations $\theta = 0^\circ, 10^\circ, 15^\circ, 30^\circ, 45^\circ, 60^\circ, 75^\circ, 80^\circ$ and 90° and with confining pressures $\sigma_3 = 0, 5, 10, 20, 30$ and 40 MPa (see Table II). The definition of the angle θ is given in Figure 1(b). In this paper, the emphasis is put on the description of the failure behaviour. Therefore, general mechanical responses

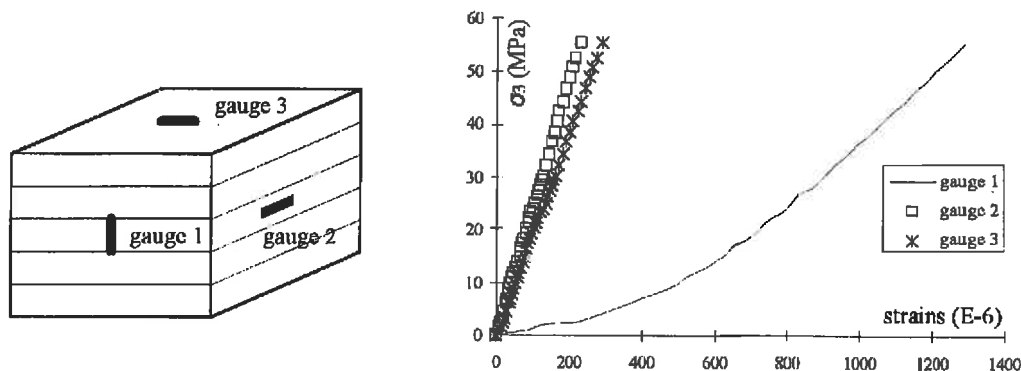


Figure 3. Experimental results of a hydrostatic compression test and positions of the strain gauges

of the schist in triaxial tests are not presented here and only a summary of failure stresses and an analysis of failure mechanisms are addressed.

Direct observations of sample failure surfaces were performed in each triaxial test. These observations have shown complex failure modes of the schist, strongly depending on the loading orientation and confining pressure (Figure 4). Main failure mechanisms of the schist can be summarized as follows:

- For the orientation $\theta = 90^\circ$, the failure occurs by strain localization in the rock matrix. Such a failure mode is widely obtained in many rocks and soils. However, in the case of the schist, the orientation of shear bands seems to be independent of confining pressure and has a quasi-constant value of 25° .
- For the orientation $\theta = 0^\circ$, the failure mode depends on confining pressure. The sample failure takes place by bursting of bedding planes under low confining pressures, while a mixed mode of bursting of bedding planes and shearing of rock matrix is obtained when the confining pressure is higher.
- For the orientations between $\theta = 30^\circ$ and $\theta = 60^\circ$, the failure is clearly dominated by sliding of bedding planes.
- For all other orientations, the failure can occur in a very complex way, by combining sliding and bursting of bedding planes and shear bands in the rock matrix.

Failure stresses are generally defined as peak stresses in triaxial tests. From the triaxial compression tests performed, the values of failure stresses of the schist are presented in Figures 5 and 6, respectively, in function of loading orientation and confining pressure. Some important remarks can be made. From Figure 5, we can notice a very strong variation of strength with the loading orientation for all confining pressures tested. However, the material strength is nearly constant for the loading orientations between $\theta = 30^\circ$ and $\theta = 60^\circ$ and increases rapidly away from this zone. This strength variation is the result of the specific failure mechanisms of the schist and is in agreement with the previously mentioned failure surfaces observed in samples. Indeed, for the loading orientations between $\theta = 30^\circ$ and $\theta = 60^\circ$, the schist failure is due to the sliding along the bedding planes and the influence of the loading orientation remains small. The sudden increases of strength at the boundaries of this zone represent the transition from the sliding of bedding plane to the shearing of rock matrix. In addition, the influence of confining pressure on the material strength is also small in this zone. However, the influence of the confining pressure is clearly more significant for loading orientation outside of this zone, particularly for $\theta = 0^\circ$ and $\theta = 90^\circ$. In these orientations, the failure, being due to the strain localization in rock matrix, is more sensitive to the confining pressure. This is a common property of most isotropic geomaterials.

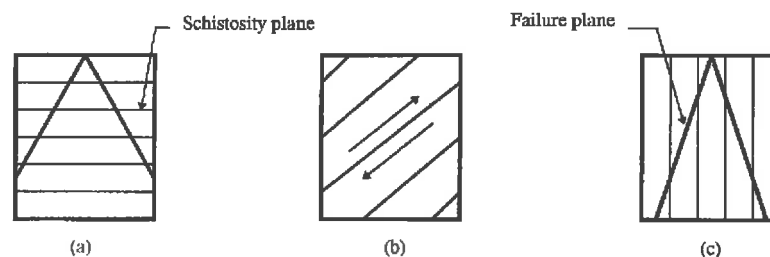
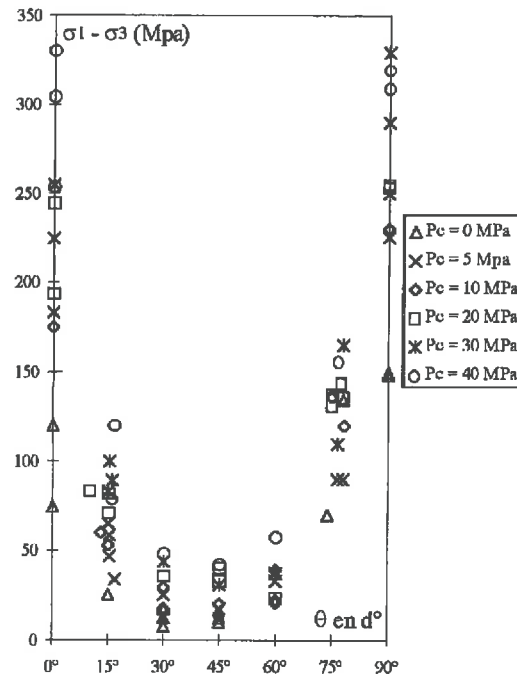
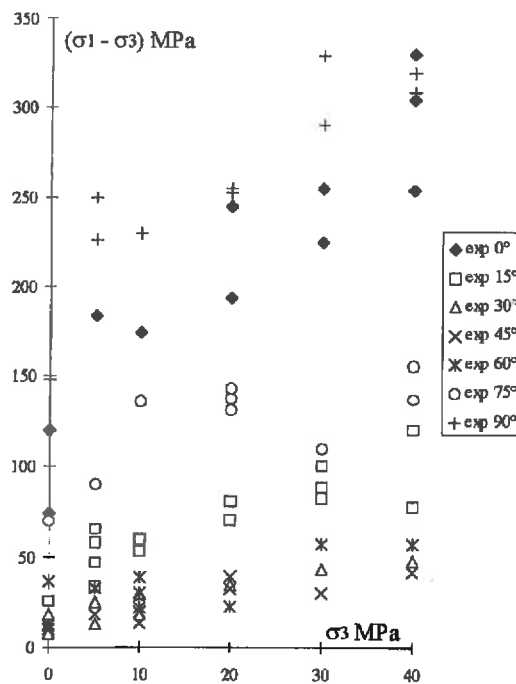


Figure 4. Schematic view of failures surfaces in samples tested: (a) $\theta = 90^\circ$ rock matrix shearing; (b) $\theta = 45^\circ$ sliding along schistosity planes; (c) $\theta = 0^\circ$ rock matrix shearing and schistosity plane bursting

Figure 5. Strength variations with the angle θ for various confining pressures testedFigure 6. Failure stresses obtained for different confining pressures and for various loading orientations θ

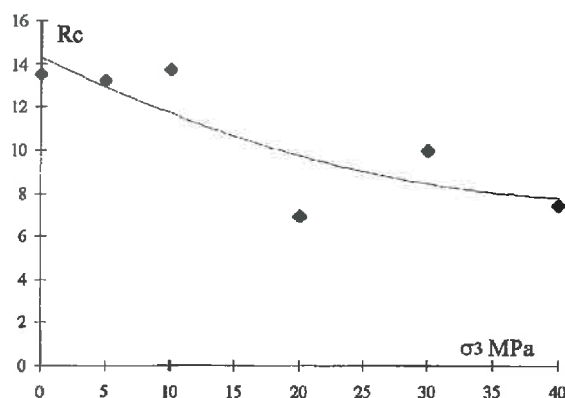


Figure 7. Evolution of the anisotropy ratio R_c with confining pressure

The degree of strength anisotropy is commonly quantified by the ratio between the biggest and smallest values of material strength for a given confining pressure. Thus, this ratio is calculated by:

$$R_c = \frac{\sigma_{c_{max i}}}{\sigma_{c_{min i}}} \quad (2)$$

Variations of this strength anisotropy with confining pressure are presented in Figure 7. The value of R_c continuously decreases with confining pressure. This means that the material anisotropy is smaller when the confining pressure is higher. However, this decrease is quite small and the strength anisotropy seems to tend towards a constant value of about eight. According to a review study by Ramamurthy,⁴¹ such a value still defines a very strong anisotropy of the material. Therefore, the effect of the confining pressure to reduce the strength anisotropy of the schist is small, with respect to results obtained for many sedimentary ductile rocks, like shale.¹⁶ Indeed, in ductile sedimentary rocks, the rupture by sliding of bedding planes is not the dominant mode, and the strength anisotropy decreases very significantly when confining pressure increases.

3. PRESENTATION AND CALIBRATION OF SOME SELECTED FAILURE CRITERIA

In this section, qualitative comparisons of some representative failure criteria are provided. All the selected models will be calibrated from the experimental data of Angers schist. A short summary of the selected models is presented, while the emphasis is put on the basic assumptions and techniques included in each model to describe the strength anisotropy. The calibration procedure associated with each model is also mentioned. According to the previous tentative classification of various approaches, nine representative criteria are selected in this work.

1. three mathematical continuous models (Pariseau,²⁰ Tasi and Wu,¹⁹ Cazacu²⁶);
2. two empirical continuous criteria (McLamore and Gray,¹⁰ Ramamurthy, Rao and Singh²⁸);
3. Four 'discontinuous weakness planes based' theories (Jaeger,³⁰ Walsh and Brace,³² Hoek,⁴² Duveau and Henry³⁵).

3.1. Mathematical continuous models

3.1.1. Criterion of Pariseau.²⁰ This theory is a straightforward extension of the anisotropic failure criterion proposed by Hill¹⁷ for cohesive frictionless materials to cohesive frictional materials. Indeed, in frictional materials like rocks and soils, mechanical behaviours are very sensitive to the mean stress. By taking into account the material anisotropy, Pariseau²⁰ introduced a linear term of three normal stresses in the Hill criterion to describe the pressure dependency. Thus, for a transversely isotropic material, and by using the structural co-ordinate system defined in Figure 1(b), the Pariseau theory is expressed by:

$$\begin{aligned} & [F(\sigma_{22} - \sigma_{33})^2 + G((\sigma_{33} - \sigma_{11})^2 + (\sigma_{11} - \sigma_{22})^2) + (2G + 4F)\sigma_{23}^2 + M(\sigma_{31}^2 + \sigma_{12}^2)]^{n/2} \\ & - [U\sigma_{11} + V(\sigma_{22} + \sigma_{33})] = 1 \end{aligned} \quad (3)$$

where F , G , M , U , V and n are six material constants involved in the criterion. σ_{ij} are the components of the stress tensor in the fixed structural system. The exponent coefficient $n \geq 1$ is used to describe a non-linear pressure dependency of strength. This is equivalent to the use of a variable friction angle in Drucker–Prager theory for isotropic media. The material constants can theoretically be determined by measuring the strengths in uniaxial tension, compression and pure shear tests in the directions normal and parallel to the bedding planes. However, the pure shear test is usually difficult to carry out in rocks, the alternative method is to use an out-of-axis uniaxial compression test (Amadei⁴³). Therefore, when $n = 1$ the following equations can be used:

$$\begin{aligned} 2V &= \frac{1}{T_{o//}} - \frac{1}{C_{o//}} & 2U &= \frac{1}{T_{op}} - \frac{1}{C_{op}} & 2G &= \frac{1}{4} \left(\frac{1}{T_{op}} + \frac{1}{C_{op}} \right)^2 \\ d2F &= \frac{1}{2} \left(\frac{1}{T_{o//}} + \frac{1}{C_{o//}} \right)^2 - 2G & M &= \left(\frac{2}{C_{45}} + U + V \right)^2 - (F + G) \end{aligned} \quad (4)$$

where T_{op} , C_{op} , $T_{o//}$, $C_{o//}$ are the uniaxial tension and compression strengths in the directions normal and parallel to the bedding planes. C_{45} is the uniaxial compression strength in the loading orientation $\theta = 45^\circ$. It is important to point out that for a strongly anisotropic rock like the schist studied, the accuracy of experimental data in uniaxial tension and compression tests are often very poor. Therefore, the above theoretical calibration procedure is actually difficult to use. In this study, only triaxial compression tests are available for the schist studied. Therefore, a numerical calibration procedure was proposed (Duveau⁴⁴). By applying the criterion (3) to triaxial tests with $\theta = 90^\circ$ and $\theta = 0^\circ$, the following simplified equations are obtained (when $n = 1$):

$$\begin{cases} \frac{1}{2}(\sigma_1 - \sigma_3)(\sqrt{8G} - 2U) - (U + 2V)\sigma_3 = 1 \\ (\sigma_1 - \sigma_3)(\sqrt{F + G} - V) - (U + 2V)\sigma_3 = 1 \end{cases} \quad (5)$$

From experimental failure stresses for different confining pressures in these two loading orientations, the parameters U , V , F , G can be determined by the least squares method. Further, the value of M can be obtained by fitting experimental failure stresses obtained in out-of-axis tests (for example $\theta = 45^\circ$). In addition, it was found that the best numerical fitting of failure stresses was obtained by taking $n = 1$. The values of material constants obtained is summarized in Table IV.

3.1.2. Criterion of Tsai and Wu.¹⁸ A general failure theory was developed by Godenblat and Kopnov¹⁸ who introduced anisotropic strength tensors of different orders. A specific form of this general theory, by ignoring strength tensors of higher order than two, was proposed by Tsai and

Table III. Major and minor anisotropies measured in three different blocks (from Homand *et al.*³⁸)

	Block A	Block B	Block C
$\Delta M\%$	28.5	30.4	27.1
$\Delta m\%$	5.4	1.0	4.2

Wu.¹⁹ Though initially developed for fibre-reinforced composites, this criterion is widely used for different kinds of materials. For a transversely isotropic material, in the structural co-ordinate system (Figure 1(a)), the Tsai and Wu¹⁹ criterion is expressed in the following form:

$$F_1\sigma_{11} + F_2(\sigma_{22} + \sigma_{33}) + F_{11}\sigma_{11}^2 + F_{22}(\sigma_{22}^2 + \sigma_{33}^2) + 2F_{12}(\sigma_{11}\sigma_{22} + \sigma_{11}\sigma_{33}) + 2F_{23}\sigma_{33}\sigma_{22} + \frac{1}{2}(F_{22} - F_{23})\sigma_{23}^2 + F_{55}(\sigma_{12}^2 + \sigma_{31}^2) = 1 \quad (6)$$

This criterion contains seven constants that can theoretically be identified from uniaxial tensile and compressive tests with $\theta = 0^\circ$ and $\theta = 90^\circ$, a pure shear test in the isotropic plane and bi-axial tensile tests. As reliable experimental data of such tests are usually unavailable, the calibration of this criterion is difficult. In this work, it was proposed to use the general theory of inverse problem (Tarantola⁴⁵) to determine the constants from failure stresses of triaxial tests. However, because of the great number of constants and the strong anisotropy of the schist, it was not possible to find a suitable set of constants. Therefore, quantitative comparisons of this criterion with experimental data will not be provided.

3.1.3. Criterion of Cazacu.²⁶ Based on the previous works of Boehler and Sawczuk,²¹ and Boehler,²⁵ Cazacu²⁶ proposed a new general invariant failure criterion for anisotropic material, by using the representation theorems of tensorial functions (Wang⁴⁶). In this criterion, a fourth order strength tensor has been introduced and used to define a transformed stress tensor from the nominal one:

$$\Sigma_{ij} = A_{ijkl}\sigma_{kl} \quad (7)$$

The strength anisotropy is taken into account by substituting the transformed tensor for the nominal one in a suitable isotropic criterion. Cazacu proposed to generalize the Stassi criterion and the anisotropic criterion is expressed in the following form:

$$\frac{3}{2}\text{tr}(\Sigma')^2 - \frac{m}{3}\text{tr}(\Sigma) = 1 \quad (8)$$

where Σ' is the deviator Σ , and m is a material constant. The tensor A has the general symmetry properties:

$$A_{ijkl} = A_{klij} = A_{jikl} = A_{ijlk} \quad (9)$$

For a transversely isotropic material and in the structural co-ordinate system, the truncated matrix of A is expressed as follows:

$$A = \begin{bmatrix} a & b & b & 0 & 0 & 0 \\ b & d & e & 0 & 0 & 0 \\ b & e & d & 0 & 0 & 0 \\ 0 & 0 & 0 & \frac{d-e}{2} & 0 & 0 \\ 0 & 0 & 0 & 0 & \frac{c}{2} & 0 \\ 0 & 0 & 0 & 0 & 0 & \frac{c}{2} \end{bmatrix} \quad (10)$$

In contrast to Boehler and Sawczuk,²¹ in Cazacu theory, the only restriction imposed on the tensor A is to be invariant under any orthogonal transformation belonging to the material symmetry group. Therefore, the tensor involves five independent components instead of three, as in the Boehler and Sawczuk theory, due to additional simplified assumptions. However, the application of a strength criterion of type (8) with A having only three independent components to some specific cases leads to unacceptably restrictive results. A detailed discussion about this point is given in Cazacu.²⁶ The tensor A given in equation (10) is similar to the elastic compliance tensor for transverse isotropic materials. Such a tensor was related by Cowin⁴⁷ to a structure tensor. Accordingly, the tensor $A : \sigma$ could physically be related to some elastic strain induced in the rock.

The physical interpretation of the parameters can be revealed from basic laboratory tests. Indeed, all the parameters are related to the material strengths in uniaxial tensile and compressive tests along the S_1 and S_2 axes, and in pure shear tests in the (S_2, S_3) plane and in the (S_1, S_2) plane (Cazacu²⁶). When such data are not fully available, a numerical fitting procedure will be necessary to determine the model's parameters. In this work, data from tensile and shear tests are not available. Thus, the parameters have been determined from triaxial compression tests, by using a numerical fitting based on the general inverse problem theory. The values obtained are presented in Table IV.

As a general remark, the presentation of the previous mathematical models could also be made in the framework of a unified formulation by using the theory of invariants. Indeed, specific forms of failure criteria could be obtained by choosing different structure tensors and invariants. However, in this paper, the initial forms of the models are used, and the emphasis is put on the physical interpretations and determination procedure of the constants involved in each model.

3.2. Empirical continuous models

Empirical continuous models have been developed in a more pragmatic way. In this class of models, an isotropic strength theory is usually generalized by introducing some empirical laws for the variations of material parameters with the loading orientation.

3.2.1. Criterion of McLamore and Gray.¹⁰ The first failure criterion of this type was proposed by Jaeger,²⁷ known as 'the variable cohesive strength theory'. It was assumed that the material failure can be described by the Mohr–Coulomb theory. In order to describe the strength anisotropy, an empirical law of variation of the material cohesion with loading orientation was proposed while the internal friction was assumed to be constant. By completing the Jaeger criterion, and in order to obtain a better description of the strength anisotropy observed in many experiments. McLamore and

Gray¹⁰ proposed to use a variable cohesion and friction coefficient with the loading orientation:

$$\tau = c + \sigma \tan \phi$$

with

$$c = A_{1,2} - B_{1,2} \cos(2(\xi_c - \theta))^n \quad (11)$$

and

$$\tan \phi = C_{1,2} - D_{1,2} \cos(2(\xi_f - \theta))^m$$

where τ is the shear stress and σ the normal stress in the Mohr plane. A_1 and B_1 , A_2 and B_2 are constants for the description of variation of the cohesion, respectively, for the loading orientations $0^\circ \leq \theta \leq \xi_c$ and $\xi_c \leq \theta \leq 90^\circ$. ξ_c is the loading orientation corresponding to the minimum cohesion. Similarly, C_1 and D_1 , C_2 and D_2 are constants for the description of variation of the friction coefficient, respectively, for the loading orientations $0^\circ \leq \theta \leq \xi_f$ and $\xi_f \leq \theta \leq 90^\circ$ where ξ_f is the loading orientation corresponding to the minimum friction. Finally, the two exponents m and n , called the factors of anisotropy type, have typical values of one to three for plane anisotropy like cleavage and schistosity, and five to six for linear structures.

The identification of the model's parameters is easy and consists of determining the values of cohesion and friction for each loading orientation by establishing the Mohr–Coulomb diagram. However, in order to have a fine description of the variation of cohesion and friction, it is necessary to perform a large series of triaxial tests covering various loading orientations θ and confining pressures. For the schist studied, the minimum cohesion and friction are found in $\theta = 45^\circ$ and $m = n = 1$ corresponds to the best fitting of the strength anisotropy. The values of parameters obtained is given in Table III. In Figure 8, experimental variations of cohesion and friction of the schist with loading orientation are presented and compared with the numerical fitting given by equations (11). Good agreements can be noticed.

3.2.2. Criterion of Ramamurthy, Rao and Singh.²⁸ Recently, a modification of the previous criterion was proposed by Ramamurthy, Rao and Singh²⁸ who suggested to use a non-linear equation to describe the failure envelope in the Mohr plane:

$$\frac{\sigma_1 - \sigma_3}{\sigma_3} = \beta \left(\frac{\sigma_c}{\sigma_3} \right)^\alpha \quad (12)$$

where σ_1 and σ_3 are the major and minor principal stresses, and σ_c the uniaxial compression strength. α and β are two parameters of the model. The material strength anisotropy is taken into account by defining the variation laws of the parameters α and β as functions of the loading orientation θ (Ramamurthy, Rao and Singh,²⁸ and Singh, Ramamurthy and Rao²⁹):

$$\frac{\alpha}{\alpha_{90}} = \left(\frac{\sigma_c}{\sigma_{c90}} \right)^{1-\alpha_{90}} \quad \frac{\beta}{\beta_{90}} = \sqrt{\frac{\alpha}{\alpha_{90}}} \quad (13a)$$

$$\begin{cases} \sigma_c = A_1 + B_1 \cos(2(\theta_{\min} - \theta)) & \text{if } \theta \leq \theta_{\min} \\ \sigma_c = A_2 + B_2 \cos(2(\theta_{\min} - \theta)) & \text{if } \theta \geq \theta_{\min} \end{cases} \quad (13b)$$

where θ_{\min} , like ξ in the McLamore and Gray model, is the loading orientation corresponding to the smallest strength. σ_{c90} is the uniaxial compression strength in $\theta = 90^\circ$, while α_{90} and β_{90} are the values of α and β in $\theta = 90^\circ$. Four constants A_1 , A_2 , B_1 and B_2 are used to describe the variations of the uniaxial compression strength as functions of loading orientation. The determination of the seven parameters is quite easy if triaxial tests for different loading orientations and confining pressures are

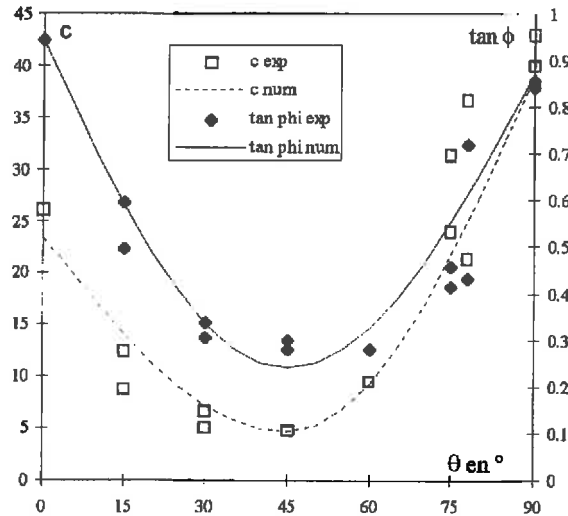


Figure 8. Experimental data of material cohesive and frictional strengths of the schist and numerical fitting from the McLamore and Gray criterion

available. The parameters σ_{c90} , α_{90} and β_{90} are obtained by plotting the failure envelope in Mohr plane from data of triaxial tests in $\theta = 90^\circ$. However, the values of A_1 , A_2 , B_1 and B_2 are determined by fitting experimental variations of the uniaxial compression strength as function θ . The values of parameters obtained for Angers schist are presented in Table III.

3.3. Discontinuous 'weakness plane based' criteria

In contrast to the previous models, in this class of models, the formulation of strength criteria is directly based on an analysis of failure mechanism. In general, an anisotropic material is, in microscopic scale, considered as an isotropic body containing some sets of weakness planes. Material failure can take place either in the rock matrix or along these weakness planes as a function of the loading orientation. Therefore, two distinct failure criteria, respectively, for rock matrix and weakness planes should be combined.

3.3.1. Single plane of weakness theory of Jaeger.³⁰ In this theory, the anisotropic material is seen as an isotropic body containing one set of weakness planes. The failure in the rock matrix and along weakness planes is together described by the Mohr–Coulomb type criterion. However, the values of cohesion and friction are different for rock matrix and weakness planes. Thus, the failure criterion is expressed by the following equations:

$$\tau = c + \sigma_n \tan \phi \quad (14)$$

$$\tau_\theta = c' + \sigma_\theta \tan \phi, \quad (15)$$

In equation (14), c and ϕ are the cohesion and friction of the rock matrix. In equation (15), τ_θ and σ_θ are, respectively, shear and normal stress applied to the weakness planes. c' and ϕ' are the cohesion and friction of weakness planes. By making use of equations (14) and (15), we obtain two values of failure stress for each orientation. The true failure stress corresponds to the smallest one of the two values, as illustrated in Figure 8.

The determination of the four material constants is quite easy. The cohesion and friction of rock matrix can be determined from failure stresses obtained in triaxial tests with $\theta = 90^\circ$ and (or) $\theta = 0^\circ$, as in these orientations, the failure takes place in the rock matrix. However, according to experimental data for many anisotropic rocks, like the Angers schist, the strength in $\theta = 90^\circ$ is clearly different from that in $\theta = 0^\circ$ (Figures 5 and 6). Therefore, it is necessary to take different values of cohesion and friction for the two principal directions. Finally, the cohesion and friction of weakness planes have to be determined from failure stresses obtained in triaxial tests in the loading orientation corresponding to the minimum strength, generally in $\theta \approx 45^\circ$. In this orientation, the material failure occurs along weakness planes. The set of parameters for the Angers schist is given in Table IV.

3.3.2. Criterion of Walsh and Brace.³² In contrast to the Jaeger theory, in the criterion of Walsh and Brace,³² it is assumed that schistosity planes represent oriented Griffith cracks. They supposed that the anisotropic body is composed of long orientated cracks (schistosity planes) that are buried in an isotropic body containing an array of randomly distributed smaller cracks. Failure occurs due to tensile stress through the growth of either the long or small cracks depending on the orientation of the long cracks with respect to the applied stress. The growth of both the long and small cracks is described by the modified Griffith theory by McClintock and Walsh:³¹

$$\tau = 2|\sigma_t| + \mu\sigma_u \quad (16)$$

Applying this theory to each system of cracks in the case of triaxial tests, we obtained the following equations describing failure stresses by growth of the long and small cracks:

$$(\sigma_1 - \sigma_3)_s = R_s + \frac{\sigma_3 \mu_s}{\sqrt{1 + \mu_s^2} - \mu_s} \quad (17)$$

$$(\sigma_1 - \sigma_3)_l = \frac{2\sigma_3 \mu_l + R_l(\sqrt{1 + \mu_l^2} - \mu_l)}{(1 - \tan \theta \mu_l) \sin 2\theta} \quad (18)$$

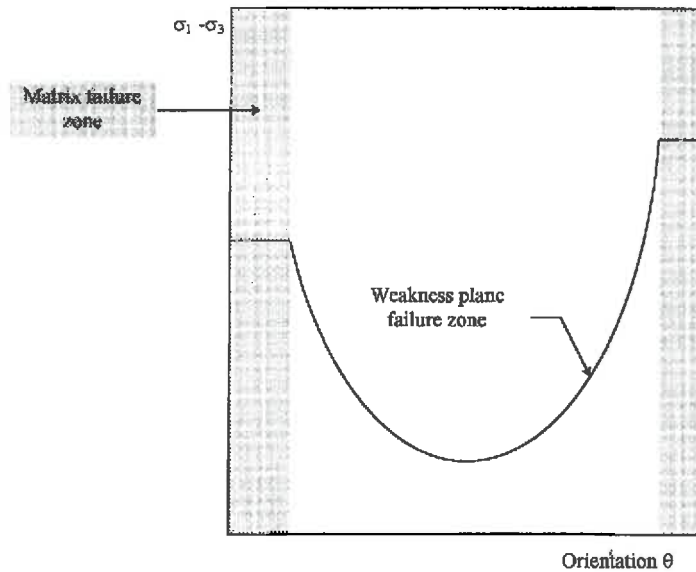


Figure 9. Schematic presentation of failure mechanisms in 'weakness plane' criteria

where R_s is the uniaxial compression strength of the isotropic body containing random small cracks only, and μ_s is the friction coefficient of the small cracks. Similarly, R_l is the uniaxial compression strength of the body with orientated long cracks only, and μ_l is the friction coefficient of the long cracks. The loading orientation θ is the angle between the major stress and the orientation of the long cracks.

The determination procedure of the material constants is similar to that used in the Jaeger theory. The constants R_s and μ_s are determined from failure stresses of triaxial tests with $\theta = 90^\circ$ and $\theta = 0^\circ$. For most anisotropic rocks, like the Angers schist, different values of R_s and μ_s are obtained for $\theta = 90^\circ$ and $\theta = 0^\circ$. The constants concerning the long cracks system, R_l and μ_l , are determined from triaxial tests with the loading orientation corresponding to the minimum strength. The values of constants for the schist studied are given in Table III.

3.3.3. Theory of Hoek.⁸ Based on the previous works of Walsh and Brace,³² and Jaeger,^{27,30} and always assuming that failure can occur either in rock matrix or along weakness planes, a more sophisticated model was proposed by Hoek.⁸ The main modification with respect to the Jaeger³⁰ theory, is the development of a new non-linear failure criterion to replace the classic Mohr–Coulomb theory. From many experimental data, Hoek and Brown^{33,34} proposed the following strength criterion:

$$\sigma_1 = \sigma_3 + (m\sigma_c\sigma_3 + s\sigma_c^2)^{1/2} \quad \text{with } \sigma_1 > \sigma_2 > \sigma_3 \quad (19)$$

where σ_c is the uniaxial compression strength of an intact rock matrix. m and s are two material constants which play the essential role in this criterion. Indeed, their values are related to the state of fractures of rock. The value of m varies from 0.001 for a very strongly fractured rock to 25 for a very hard intact rock, while the value of s varies from 0 to 1. From equation (19), it is possible to obtain a Mohr–Coulomb type criterion with variable cohesion and frictional angle as a function of the normal stress σ_n (Hoek^{8,42}):

$$\tau = c^*(m, s; \sigma_n) + \sigma_n \tan \phi^*(m, s, \sigma_n) \quad (20)$$

In order to apply the criterion (19) to an anisotropic materials containing one set of weakness planes, it was proposed to use different values of m and s , respectively, for intact rock matrix and weakness planes. The failure in rock matrix is directly described by equation (19). However, for the description of sliding along the schistosity planes, equation (20) was used with the corresponding values of m and s , denoted m_j and s_j . Accordingly, τ and σ_n in equation (20), are, respectively, the shear stress and the normal stress applied on the schistosity plane. Therefore, by assuming $s = 1$ for rock matrix (in fact, is impossible to have a real intact rock mass as all rocks contain some distribution of cracks), the uniaxial compression strength σ_c and m are easily obtained from failure stresses of triaxial tests with $\theta = 90^\circ$ and $\theta = 0^\circ$. However, the constants for weakness planes, m_j and s_j , are determined from triaxial tests in the loading orientation corresponding the minimum strength.

3.3.4. Criterion of Duveau and Henry.³⁵ Similarly to the previous theories of Jaeger,³⁰ Walsh and Brace,³² and Hoek,⁸ this criterion is also based on the weakness planes concept. However, according to experimental observations, the schist of Angers has very marked schistosity planes and their behaviour seems to be similar to that of rock joints. The classic Mohr–Coulomb or McClintock and Walsh³¹ criterion was found not to be suitable to describe the failure along such schistosity planes. Therefore, Duveau and Henry³⁵ proposed to adapt the criterion of Barton⁴⁸ initially developed for

rock joints:

$$\tau = \sigma_n \tan \left(\text{alog} \frac{\sigma_{c0}}{\sigma_n} + b \right) \quad (21)$$

where σ_{c0} is the uniaxial compression stress in the direction normal to schistosity planes. It is equivalent to the initial definition of the parameter JCS (joint compression strength) in the Barton model. a and b are two other constants of the model. τ and σ_n are, respectively, the shear and normal stress applied to schistosity planes.

The failure in rock matrix is described by the tri-dimensional criterion of Lade.⁴⁸

$$\left(\frac{I_1^*}{I_3^*} - 27 \right) \left(\frac{I_1^*}{P_r} \right)^m - Y_{dr} = 0 \quad (22)$$

with

$$\begin{cases} I_1^* = \sigma_1 + \sigma_2 + \sigma_3 + 3c \\ I_3^* = (\sigma_1 + c)(\sigma_2 + c)(\sigma_3 + c) \end{cases} \quad (24)$$

where m , c and Y_{dr} are three material constants and P_r is a reference pressure in order to obtain undimensional constants.

The determination of all the parameters is quite easy. The constants concerning failure along schistosity planes are determined from out-of-axis triaxial tests in the loading orientation corresponding to the minimum strength. The parameters concerning matrix failure should be determined from triaxial tests with $\theta = 90^\circ$ and $\theta = 0^\circ$. It was found that different values of m and Y_{dr} have to be used for the principal directions. The obtained values are presented in Table IV.

4. COMPARISONS AND DISCUSSIONS

In the previous section, the formulation and calibration of nine criteria that are representative of three different approaches, are presented. The values of the parameters involved in each model are summarized in Table IV. Using these values, the models are now applied to simulate the strength of the schist of Angers. In this section, comparisons of numerical simulations from each model with experimental data are presented. General discussions about the performance of each criterion are addressed.

From a qualitative point of view, the three approaches use different assumptions and techniques to take into account the strength anisotropy. Based on the overall analysis of mechanical behaviours of materials, mathematical continuous models propose a general and rigorous procedure by making use of anisotropic strength tensor. These models provide an invariant formulation with respect to the material symmetry groups. Their calibration requires a small number of laboratory tests, and their numerical implementation is easy and robust. However, the theoretical calibration procedure proposed in these models cannot practically be used because the laboratory tests required are usually impossible to carry out. A numerical optimal fitting method is often necessary. In addition, for rocks with strong anisotropy, like the schist studied, these models cannot account for the discontinuous character of the transition from the rock-matrix failure to the schistosity-plane sliding. Therefore, these models generally give too smooth a variation of material strength. However, these models may give an excellent modelling of failure behaviour of weakly anisotropic materials when the influence of weakness planes is not dominant.²⁶

Empirical continuous models provide a rudimentary adaptation of isotropic strength criteria to anisotropic material, by proposing empirical variation laws of model parameters with loading

orientation. These models lead to a simple mathematical form and the determination of the model's parameters is easy. However, the physical meanings of the empirical laws and the involved parameters are not clear. The application of these models are generally limited to the 2D case. In addition, a high number of laboratory tests is needed to obtain reliable variation laws. For a material with strong bedding planes, these models suffer the same shortcomings as the mathematical continuous models.

In contrast to the continuous models, the 'discontinuous weakness planes' based models consider that the material strength is inherently related to the presence of bedding planes. The final material failure is the result of two distinct mechanisms in the microscopic level; isotropic failure in rock matrix and orientated failure along weakness planes. These models lead to simple and physically-based equations. In addition, these models contain a small number of parameters and their determination is generally easy. These models are obviously well suited to a material with strong anisotropy. However, these models do not provide an invariant formulation with respect to the material symmetries, and their numerical implementation in the 3D case is not easy. Furthermore, for weakly anisotropic materials, their advantages with respect to the mathematical continuous models will be reduced.

Quantitative comparisons of numerical simulations from the selected models with experimental data are presented in Figures 10 to 17. Variations of the deviatoric failure stress in triaxial tests with loading orientation are shown for two representative values of the confining pressure; 5 and 40 MPa.

In Figure 10, we can notice a quite good agreement between the numerical results from the Pariseau²⁰ criterion and experimental data. Particularly, this criterion seems to describe well the weak strength anisotropy for the loading orientations $\theta \in [30^\circ, 60^\circ]$. However, if the material strength for the orientations near to $\theta = 0^\circ$ is correctly simulated, there is a significant difference between the numerical and experimental results for the orientations near to $\theta = 90^\circ$. This seems to confirm the previous qualitative analysis of this model.

In Figure 11, the numerical values of failure stresses from the Cazacu²⁶ criterion are compared with data. In a general way, the quality of the numerical predictions is not good. This model does not

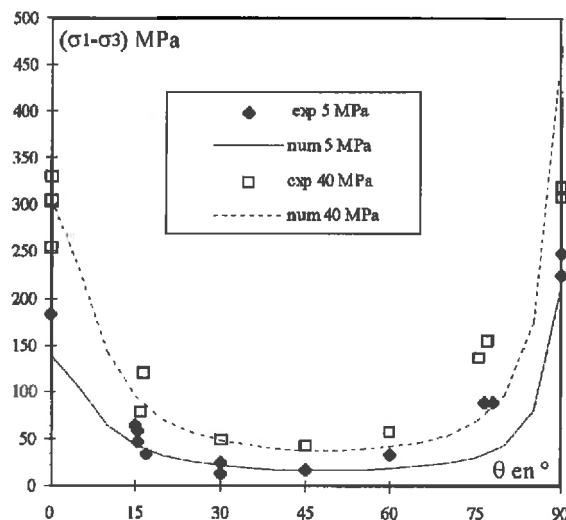


Figure 10. Comparison of the calculated strength values from Pariseau's criterion with the experimental triaxial data for two representative confining pressures ($P_c = 5$ MPa and $P_c = 40$ MPa)

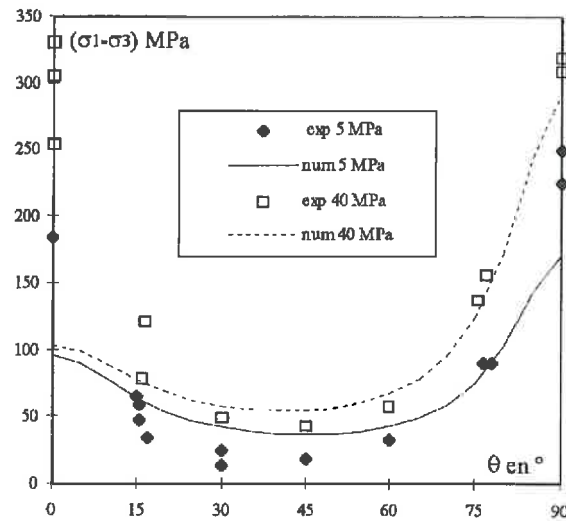


Figure 11. Comparison of the calculated strength values from Cazacu's criterion with the experimental triaxial data for two representative confining pressures ($P_c = 5$ MPa and $P_c = 40$ MPa)

correctly describe three distinct strength zones observed in experimental data and gives too smooth an anisotropy of strength. Therefore, this model suffers the same kind of shortcomings as the Pariseau model.

In Figures 12 and 13, the numerical results given by making use of the two empirical continuous models (McLamore and Gray,¹⁰ and Ramamurthy, Rao and Singh²⁸) are compared with data. From a quantitative point of view, we can notice very good agreement for the McLamore and Gray model, and less good agreement for the Ramamurthy, Rao and Singh model. However, the good numerical

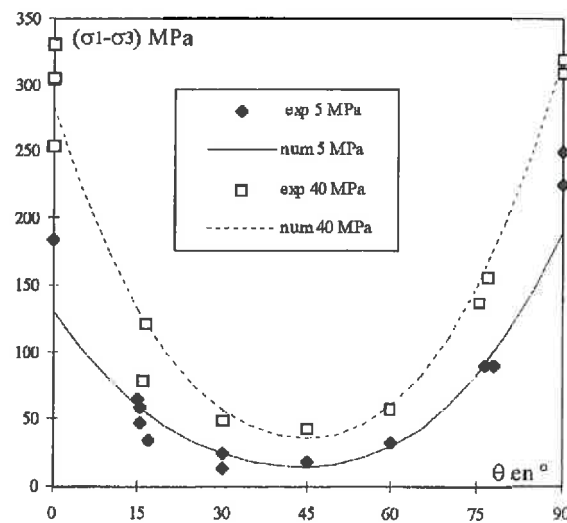


Figure 12. Comparison of the calculated strength values from McLamore and Gray's criterion with the experimental triaxial data for two representative confining pressures ($P_c = 5$ MPa and $P_c = 40$ MPa)

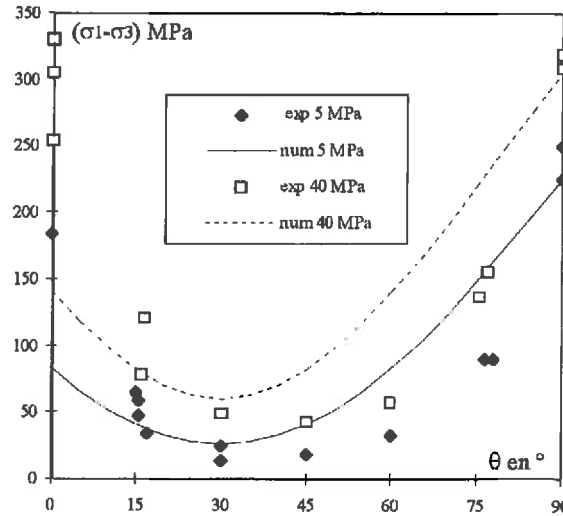


Figure 13. Comparison of the calculated strength values from Ramamurthy, Rao and Singh's criterion with the experimental triaxial data for two representative confining pressures ($P_c = 5$ MPa and $P_c = 40$ MPa)

performance of these models is not significant. Indeed, in the case of the McLamore and Gray model, the comparisons shown in Figure 12 represent a simple verification of the used empirical laws, as all the tests simulated were used to calibrate these laws. In addition, the quality of predictions given by these models directly depends on the reliability of the empirical laws used. In conclusion, because of the lack of a clear physical and mathematical background, the empirical models are not suitable for a proper modelling of failure behaviour of anisotropic materials.

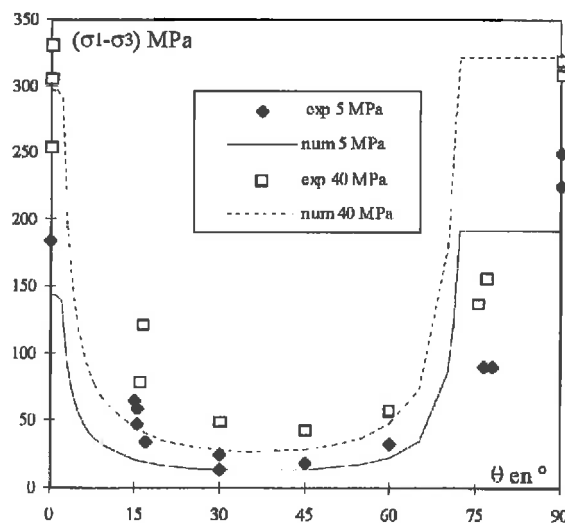


Figure 14. Comparison of the calculated strength values from Jaeger's criterion with the experimental triaxial data for two representative confining pressures ($P_c = 5$ MPa and $P_c = 40$ MPa)

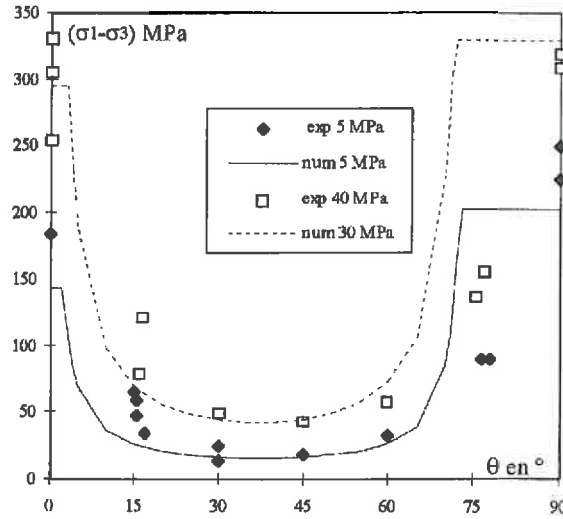


Figure 15. Comparison of the calculated strength values from Walsh and Brace's criterion with the experimental triaxial data for two representative confining pressures ($P_c = 5$ MPa and $P_c = 40$ MPa)

In Figures 14 to 17, we present the numerical results obtained from four 'discontinuous weakness planes based' models. As similar basic assumptions are used in these models, the numerical results are also similar to each other. The common point is the existence of three distinct strength zones; two constant strength 'shoulders' for the loading orientations near to the principal directions $\theta = 0^\circ$ and $\theta = 90^\circ$, and a variable strength zone for other orientations. The boundaries between different strength zones represent the transition from rock matrix failure to weakness planes rupture. Never-

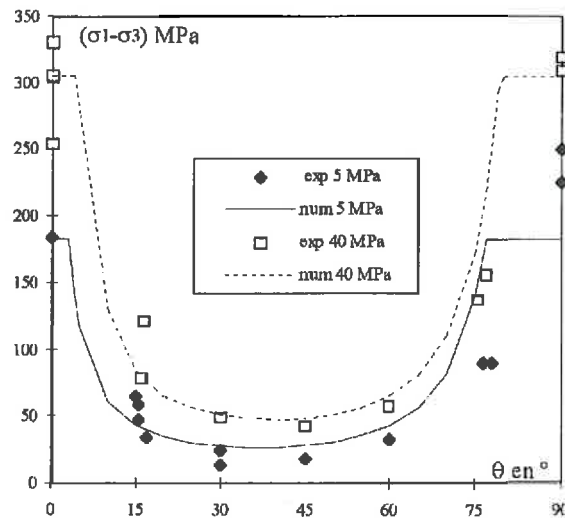


Figure 16. Comparison of the calculated strength values from Hoek's criterion with the experimental triaxial data for two representative confining pressures ($P_c = 5$ MPa and $P_c = 40$ MPa)

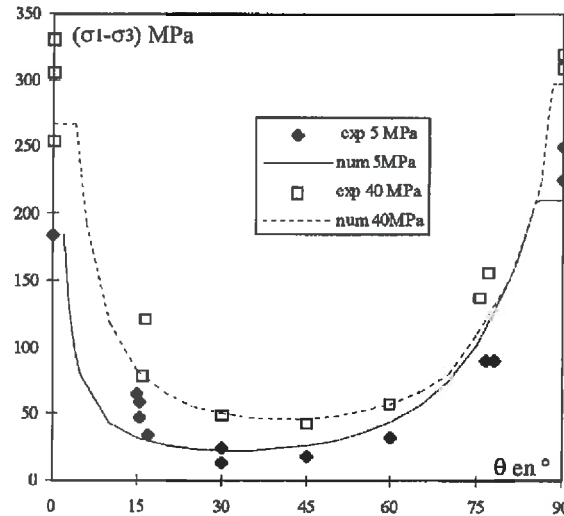


Figure 17. Comparison of the calculated strength values from Duveau and Henry's criterion with the experimental triaxial data for two representative confining pressures ($P_c = 5$ MPa and $P_c = 40$ MPa)

theless, it is useful to point out that the distinction of two failure mechanisms may appear too simplistic and does not account for more complex coupled mechanisms. However, general good agreement are obtained between the numerical and experimental results for all the models. In addition, these models describe correctly the values of the orientation corresponding to the transition from rock matrix failure to bedding plane failure. Obviously, the 'discontinuous weakness planes based' models appear particularly suitable for strongly anisotropic rocks where bedding planes play a dominant role. By comparing the numerical results of the four models and the associated parameters number (see Table IV), the Hoek⁸ criterion (four parameters used) appears to be the most attractive. If we look at the material strength in the zone corresponding to sliding of schistosity planes, it seems that the Duveau and Henry³⁵ criterion gives the closest results to the laboratory data.

Parallel to the study of strength anisotropy, the failure mode and the orientation of failure planes (angle between the major stress and the failure plane) and also analysed. In the general framework of the failure by strain localization in geomaterials, the study of the orientation of failure planes can be performed by using the bifurcation theory associated with an appropriate constitutive model. This is not the purpose of the present work. However, by assuming a brittle elastic behaviour of the material, it is possible to obtain a primary estimation of the failure planes orientation for the models used in this paper, by calculating the mobilized friction angle at failure state. One model of each group is chosen. Comparisons between the predicted and observed values are shown in Table V. For the loading orientations between 15 and 78 degrees, the observed values from tested samples indicate that the sample failure is caused by the sliding of schistosity planes, and thus, the failure angle coincides with the loading orientation. The failure mode is inherently modelled by the 'weakness plane' based models (represented by Hoek's model). However, the continuous models give variable failure angles that obviously differ from the observed values. For the loading orientations near to the principal directions, Hoek's model provides, once again, an excellent prediction of the failure angle and the dependency of the failure angle with the confining pressure. The values given by two continuous models are also in good agreement with the observed values. But, in the case of the Pariseau model and the McLamore-Gray model, the influence of the confining pressure is not taken

Table IV. Calibration results of the selected criteria from the data of Angers schist

Criteria	Pariseau ²⁰	Cazacu ²⁶	McLamore and Gray ¹⁰	Ramamurthy, Rao and Singh ²⁸	Jaeger ³⁰	Walsh and Brace ³²	Hoek ⁸	Duveau and Henry ³⁵
Parameters used	F, G, M, U, V, N	a, b, c, d, e, m	$A_1, B_1, C_1, D_1, A_2, B_2, C_2, D_2, m, n$	$A_1, B_1, A_2, B_2, \sigma_{c90}, \alpha_{90}, \beta_{90}$	$c_0, \tan \phi_0, c_{90}, \tan \phi_{90}, c', \tan \phi'$	$R_{s0}, \mu_{s0}, R_{s90}, \mu_{s90}, R_f, \mu_f$	m, s, σ_c, m_j, s_j	$c_0, Pr, m_0, Y_{d0}, m_{90}, Y_{d90}, a, b, \sigma_{c0}$
Calibration procedure	Numerical fitting from triaxial tests with $\theta = 0^\circ, 45^\circ$ and 90° and all confining pressures tested	Numerical fitting from triaxial tests with all orientations and all confining pressures tested, by using the general inverse theory	Numerical fitting from triaxial tests with all orientations and all confining pressures tested	Numerical fitting from triaxial tests with $\theta = 0^\circ, 45^\circ$ and 90° and all confining pressures tested	Numerical fitting from triaxial tests with $\theta = 0^\circ, 45^\circ$ and 90° and all confining pressures tested	Numerical fitting from triaxial tests with $\theta = 0^\circ, 45^\circ$ and 90° and all confining pressures tested	Numerical fitting from triaxial tests with $\theta = 0^\circ, 45^\circ$ and 90° and all confining pressures tested	Numerical fitting from triaxial tests with $\theta = 0^\circ, 45^\circ$ and 90° and all confining pressures tested
Value of parameters	$n = 1$ $F = 8.8\text{E-}04 \text{ MPa}^{-2}$ $G = 9.6\text{E-}06 \text{ MPa}^{-2}$ $M = 0.0237 \text{ MPa}^{-2}$ $U = -0.012 \text{ MPa}^{-1}$ $V = 0.0212 \text{ MPa}^{-1}$	$a = 0.0195 \text{ MPa}^{-1}$ $b = 0.0058 \text{ MPa}^{-1}$ $c = 0.0485 \text{ MPa}^{-1}$ $d = -0.0357 \text{ MPa}^{-1}$ $e = 0.0081 \text{ MPa}^{-1}$ $m = 2.0376 \text{ MPa}^{-1}$	$m = n = 1$ $A_2 = 0.87$ $B_2 = -0.63$ $C_2 = 39.02$ $D_2 = -34.415$ $A_1 = 0.94$ $B_1 = -0.70$ $C_1 = 23.39$ $D_1 = -18.78$	$A_1 = 91.32$ $B_1 = -88.55$ $A_2 = 159.66$ $B_2 = -156.86$ $\sigma_{c90} = 150 \text{ MPa}$ $\alpha_{90} = 0.855$ $\beta_{90} = 2.34$	$c_0 = 26.10$ $\tan \phi_0 = 0.94$ $c_{90} = 40.04$ $\tan \phi_{90} = 0.86$ $c' = 4.01$ $\tan \phi' = 0.30$	$R_{s0} = 121.06 \text{ MPa}$ $\mu_{s0} = 0.94$ $R_{s90} = 185.07 \text{ MPa}$ $\mu_{s90} = 0.84$ $R_f = 11.71 \text{ MPa}$ $\mu_f = 0.29$	$m = 10.80$ $s = 1$ $\sigma_c = 158 \text{ MPa}$ $m_j = 0.27$ $s_j = 0.32$	$Pr = 1\ 000 \text{ MPa}$ $c = 1 \text{ MPa}$ $m_0 = 3.00$ $Y_{d0} = 5.97$ $m_{90} = 5.07$ $Y_{d90} = 1.35$ $a = 29.12$ $b = 9.29$ $\sigma_{c0} = 150 \text{ MPa}$

Table V. Comparison between observed and predicted failure angle β for different criteria

Failure mode				Rock matrix		Schistosity plane					Rock matrix	
θ				near 0°		15°	30°	45°	60°	75°	78°	near 90°
β observed				Varies with confining pressure from 15° to 20°		$\beta \approx 0$					About 25° (increase slightly with confining pressure)	
Pariseau ²⁰				22.6°		32.4°	37°	38.3°	37.8°	34.8°	33.4°	19°
McLamore and Gray ¹⁰				23.3°		29.7°	35.8°	38.3°	36°	30.5°	29.3°	24.5°
Predicted β from three models	Hoek ⁶	σ_3 (MPa)	0	21.6°		$\beta = 0$					21.6°	
			5	22.8°							22.8°	
			10	23.8°							23.8°	
			20	25.2°							25.2°	
			30	26.3°							26.3°	
			40	27.2°							27.2°	

into account. However, in other continuous models (Tsai and Wu, Cazacu, Ramamurthy, Rao and Singh), this dependency can be considered.

As in isotropic materials, the effect of the intermediate stress on the failure of anisotropic materials should be considered. However, the experiments of this work were performed on cylindrical samples under axisymmetric stress. Therefore, this topic is not discussed in this paper. However, a review of the previous works on this topic is presented by Kwasniewski.⁵⁰

In order to complete the comparative discussions, it appears important to point out that the present work is devoted to the analysis of the brittle failure behaviour of an anisotropic rock mass as a continuous medium. Although the sliding of schistosity planes is considered in the group 3 models, this was done to give a clear microscopic interpretation of the failure mode, not to provide a modelling of individual weakness planes. On a larger scale, when we need to study the stability of rock massifs containing macroscopic discontinuities (joints and fractures), two numerical modellings, respectively, for rock mass and macroscopic discontinuities, should be necessary.

5. CONCLUSION

From the assessment of nine different failure criteria in the framework of modelling the failure behaviour of strongly anisotropic materials, some concluding remarks can be drawn. Among three kinds of approaches, the empirical continuous models are based on fully empirical variation law and formulated without any physical and mathematical foundation. These models should not be recommended. However, the mathematical continuous models present a considerable advantage of providing an invariant formulation and rigorous mathematical development. In the case of strongly anisotropic materials, these models do not describe correctly the consequences of the existence of two main failure mechanisms. Finally, the 'discontinuous weakness planes' models are based on the description of two clearly identified failure modes, and thus, are especially suitable for strongly anisotropic materials. However, these models do not provide an invariant formulation and their numerical implementation is not easy.

REFERENCES

1. F. A. Donath, 'Experimental study of shear failure in anisotropic rocks', *Geol. Soc. Am. Bull.*, **72**, 985 (1961).
2. F. A. Donath, 'Strength variation and deformational behavior in anisotropic rock', in *State of Stress in the Earth's Crust*, W. R. Judd ed., Elsevier, Amsterdam, p. 281, 1964.
3. F. A. Donath, 'Effects of cohesion and granularity on deformational behavior of anisotropic rock', in *Studies in Mineralogy and Precambrian Geology*, B. R. Doc and D. K. Smith eds., vol. 135, p. 95, Geological Society of America, Boulder, CO, 1972.
4. F. A. Donath and C. I. Cohen, 'Experimental study of shear failure in anisotropic rocks (abstract)', *Geol. Soc. Am. Bull.*, **71**, 1851 (1960).
5. M. Dayre and P. Sirieys, 'Anisotropie des modules élastiques et des résistances à la rupture des roches métamorphiques', *C.R. Acad. Sci., Paris*, **260**, 4040 (1965).
6. E. Hoek, 'Fracture of anisotropic rock', *J. S. Afr. Inst. Min. Metall.*, **64** (10), 501 (1964).
7. E. Hoek, 'Brittle failure of rock', in *Rock Mechanics in Engineering Practice*, G. Stagg and O. C. Zienkiewicz eds., Wiley, London, p. 99, 1968.
8. E. Hoek, 'Strength of jointed rock masses', *Geotechnique*, **33** (3), 187 (1983).
9. M. E. Chenevert and C. Gatlin, 'Mechanical anisotropies of laminated sedimentary rocks', *Soc. Geol. Eng.*, **15**, 67 (1965).
10. R. McLamore and K. E. Gray, 'The mechanical behavior of anisotropic sedimentary rocks', *J. of Engineering for Industry, Trans. of the A.S.M.E.*, **89**, 62 (1967).
11. P. B. Attewell and M. R. Sandford, 'Intrinsic shear strength of a brittle anisotropic rock.—I: experimental and mechanical interpretation', *Int. J. Rock Mech. Min. Sci. & Geomech. Abstr.*, **11**, 423 (1974).
12. C. Saint Leu, J. Lerau and P. Sirieys, 'Mécanisme de rupture des schistes de lacaune (Tarn). Influence de la pression isotrope', *Bull. Soc. Fr. Min. Cristal*, **10**, p. 437 (1978).
13. D. Alliot and J. P. Boehler, 'Evolution des propriétés mécaniques d'une roche stratifiée sous pression de confinement', in *Proc. 4th Int. Soc. Rock Mech.*, Montreaux, Balkema, Rotterdam, vol. 1, p. 15 (1979).

14. P. Sirieys 'Anisotropie mécanique des roches', *Colloque Int. du C.N.R.S. sur le comportement mécanique des solides anisotropes*, **295**, 481 (1979).
15. J. Lerou, C. Saint Leu and P. Sirieys, 'Anisotropie de la dilatance des roches schisteuses', *Rock Mechanics*, **13**, 185 (1981).
16. H. Niandou, J. F. Shao, J. P. Henry and D. Fourmaintraux, 'Laboratory investigation of the mechanical behaviour of Tournemire shale', *Int. J. Rock Mech. & Min. Sci.*, **34** (1), 3–16 (1997).
17. R. Hill, *The Mathematical Theory of Plasticity*, Oxford University Press, Oxford, 1950.
18. I. I. Godenblat and V. A. Kopnov, 'Strength of glass-reinforced plastics in the complex stress state', *Polymer Mechanics*, **1**, 54 (1966).
19. S. W. Tsai and E. Wu, 'A general theory of strength of anisotropic materials', *J. Composite Materials*, **5**, 58 (1971).
20. W. G. Pariseau, 'Plasticity theory for anisotropic rocks and soils', *Proc. 10th Symp. on Rock Mech.*, vol. 1, AIME, p. 267, 1972.
21. J. P. Boehler and A. Sawczuk, 'Equilibre limite des sols anisotropes', *J. de Mécanique*, **5**, 5 (1970).
22. J. P. Boehler and A. Sawczuk, 'On yielding of orientated solids', *Acta Mechanica*, **27**, 185 (1977).
23. J. P. Boehler, 'Anisotropic linear elasticity', in *Application of Tensors Functions in Solid Mechanics*, Courses and Lectures, no. 292, J. P. Boehler ed., CISM Udine, 1987.
24. J. P. Boehler and J. Raclin, 'Ecouissage anisotrope des matériaux orthotropes préformés', *J. de Mécanique Théorique et Appliquée*, Numéro spécial, Janvier–Février (1982) pp. 23–44.
25. J. P. Boehler, 'Contributions théoriques et expérimentales à l'étude des milieux plastiques anisotropes', Thèse de Doctorat ès Sciences, Grenoble, 1975.
26. O. Cazacu, 'Contribution à la modélisation du comportement élasto-viscoplastique des roches anisotropes', Thèse de Doctorat U.S.T.L., 1995.
27. J. C. Jaeger, 'Friction of rocks and stability of rock slope', *Geotechnique*, **21** (2), 97 (1971).
28. T. Ramamurthy, G. V. Rao and J. A. Singh, 'A strength criterion for anisotropic rocks', *Proc. 5th Australia–New Zealand Conf. on Geomechanics*, Sydney, vol. 1, p. 253, 1988.
29. J. A. Singh, T. Ramamurthy and G. V. Rao, 'Strength anisotropies in rocks', *Indian Geotech. J.*, **19**, 147 (1988).
30. J. C. Jaeger, 'Shear failure of anisotropic rocks', *Geol. Mag.*, **97**, 65 (1960).
31. M. A. McClintock and J. B. Walsh, 'Friction on Griffith's cracks in rocks under pressure', *Proc. 4th U.S. Nat. Congress of Applied Mechanics*, vol. II, A.S.M.E., p. 1015, 1962.
32. J. B. Walsh and J. F. Brace, 'A fracture criterion for brittle anisotropic rock', *J. of Geophysical Research*, **69** (16), 3449 (1964).
33. E. Hoek and E. T. Brown, *Underground Excavations in Rock*, The Institution of Mining and Metallurgy, London, 1980.
34. E. Hoek and E. T. Brown, 'Empirical strength criterion for rock masses', *J. of the Geotech. Eng. Div., A.S.C.E.*, **106** (GT9), 1013 (1980).
35. G. Duevaux and J. P. Henry, 'Modélisation du comportement à la rupture d'un schiste ardoisier', *Revue Française de Géotechnique*, to appear (1997).
36. A. Hamade, E. Morel and J. P. Henry, 'Etude d'un modèle de comportement simplifié', Rapport ANDRA 623 R.P.L.M.L. 90-01, 1990, University of Lille.
37. A. Hamade, 'Etude expérimentale du comportement d'un matériau anisotrope (schiste ardoisier): caractérisation de la rupture et détermination des paramètres élastiques', Thèse de Doctorat, U.S.T.L., 1992, Lille, France.
38. F. Homand, E. Morel, J. P. Henry, P. Cuxac and A. Hammade, 'Characterization of the moduli of elasticity of an anisotropic rock using dynamic and static methods', *Int. J. Rock Mech. Min. Sci. & Geomech. Abstr.*, **30**, 527 (1993).
39. P. Cuxac, 'Propagation et atténuation des ondes ultrasoniques dans des roches fissurées et anisotropes', Thèse de Doctorat I.N.P.L. (E.N.S.G. Nancy), 1991.
40. J. Guyader and A. Denis, 'Propagation des ondes dans les roches anisotropes sous contraintes. Evaluation de la qualité des schistes ardoisiers', *Bull. Ass. Int. Geol. Ing.*, **33**, 49 (1986).
41. T. Ramamurthy, 'Strength and modulus responses of anisotropic rocks', in *Comprehensive Rock Engineering*, vol. 1: *Fundamentals*, J. Hudson ed., Pergamon Press, Oxford, p. 313, 1993.
42. E. Hoek, 'Estimating Mohr–Coulomb friction and cohesion values from the Hoek–Brown failure criterion', *Int. J. of Rock Mech. Min. Sci. & Geomech. Abstr.*, **27** (3), 227 (1990).
43. B. Amadei, *Rock Anisotropy and the Theory of Stress Measurements*, Springer-Verlag, Heidelberg, 1983.
44. G. Duveau, 'Contribution à la modélisation du comportement d'une roche anisotrope fragile: le schiste d'Angers', Thèse de Doctorat, U.S.T.L., 1996, Lille, France.
45. A. Tarantola, *Inverse Problem Theory* Elsevier, New York, 1987.
46. C. C. Wang, 'Corrigendum 43', *Arch. Rat. Mech. Anal.*, **36**, 392 (1971).
47. S. C. Cowin, 'The relationship between the elasticity tensor and the fabric tensor', *Mech. Mat.*, **4**, 137 (1985).
48. N. Barton, 'The shear strength of rock and rock joints', *Int. J. Rock Mech. Min. Sci. & Geomech. Abstr.*, **13**, 255 (1976).
49. P. V. Lade, 'Three parameters failure criterion for concrete', *J. Eng. Mech. Division, A.S.C.E.*, **104** (EM5), 850 (1982).
50. M. A. Kwasniewski, 'Mechanical behaviour of anisotropic rocks', in *Comprehensive Rock Engineering*, vol. 1: *Fundamentals*, J. Hudson ed., Pergamon Press, Oxford, p. 285, (1993).
51. R. von Mises, 'Mechanik der plastischen Formänderung von Kristallen', *Z. Angew. Math. Mech.*, **8**, 161 (1928).
52. W. Olszak and W. Urbanovitch, 'The plastic potential and the generalized energy in theory of non-homogeneous and anisotropic elastic–plastic bodies', *Arch. Mech. Stos.*, **8**, no. 4, 671–694 (1956).
53. I. I. Goldenblat, *Some Problems of Mechanics of Deformable Media*, Noordhoff, Gröningen, 1962.

54. Y. F. Dafalias, 'Anisotropic hardening of initially orthotropic materials', *ZAMM*, **59**, 437 (1979).
55. Y. F. Dafalias, 'Anisotropic critical state clay plasticity model', in *Constitutive Laws for Engineering Materials. Theory and Applications*, C. S. Desa *et al.* eds., Elsevier Science Publishing Co., Inc., 1987. Tucson, USA.
56. R. Nova and G. A. Sacchi, 'A generalized failure condition for orthotropic solids', *Euromech 115—Mechanical Behavior of Anisotropic Solids*, Boehler (Ed), France, June 1979, Editions of CNRS and Martinus Nijhoff (1982), 623–641.
57. R. Nova, 'The failure of transversely isotropic rocks in triaxial compression', *Int. J. Rock Mech. Min. Sci. & Geomech. Abstr.*, **17** (6), 325 (1980).
58. R. Nova, 'An extended Cam-Clay model for soft anisotropic rocks', *Computer and Geotechnics*, **2**, 69 (1986).
59. J. Raclin, 'Contributions théoriques et expérimentales à l'étude de la plasticité, de l'écroutissage et de la rupture des solides anisotropes', Thèse de Docteur ès Sciences, Grenoble, 1984.
60. D. G. Kaar, F. P. Law, M. Fatt Hoo and G. F. N. Cox, 'Asymptotic and quadratic failure criteria for anisotropic materials', *Int. J. of Plasticity*, **7**, 303 (1989).
61. A. Casagrande and N. Carrillo, 'Shear failure of anisotropic materials', *J. of Boston Soc. of Civil Eng.*, **31** (4), 122 (1944).
62. S. A. F. Murrell, 'The effect of triaxial stress system on the strength of rock at atmospheric temperature', *Int. J. Rock Mech. Min. Sci. & Geomech. Abstr.*, **3**, 11 (1965).
63. K. Barron, 'Brittle failure initiation in and ultimate failure of rocks', *Int. J. Rock Mech. Min. Sci. & Geomech. Abstr.*, **8** (6), 553 (1971).
64. B. Ladanyi and G. Archambault, 'Evaluation de la résistance au cisaillement d'un massif rocheux fragmenté', *Proc. 24th Int. Geol. Congress*, Montreal, section 13D, p. 249, 1972.
65. Z. T. Bieniawski, 'Estimating the strength of rock materials' in *J. S. Afr. Inst. Min. Metall.*, **74** (8), 312 (1974).